Food & Function

ROYAL SOCIETY OF CHEMISTRY

PAPER

View Article Online
View Journal | View Issue

Cite this: *Food Funct.*, 2022, **13**, 6623

Serum untargeted metabolomics analysis of the mechanisms of evodiamine on type 2 diabetes mellitus model rats

Yuejie Yu, †[a] Qinyan Lu,†[a] Feng Chen,[a] Shangli Wang,[a] Chunxiang Niu,[a] Jiabao Liao,[a] Hongwu Wang*[b] and Fengjuan Chen*[a]

Evodiamine (EVO) is an alkaloid extracted from *Evodia rutaecarpa* and has various pharmacological activities, including hypolipidemic, anti-inflammatory, anti-infective, and antitumor effects. However, the therapeutic effects of EVO on type 2 diabetes mellitus (T2DM) and the possible mechanisms remain unknown. In this study, we used a T2DM rat model using a high-fat diet (HFD) combined with streptozotocin (STZ) injections followed by treatment with EVO. First, we evaluated the therapeutic effects of EVO on T2DM rats, following which we evaluated the anti-inflammatory and anti-oxidative effects of EVO on T2DM rats. Finally, we analyzed the metabolic regulatory mechanism of EVO in T2DM rats using an untargeted metabolomics approach. The results showed that EVO treatment alleviated the hyperglycemia, hyperlipidemia, insulin resistance (IR), and pathological changes of the liver, pancreas and kidneys in T2DM rats. Moreover, EVO treatment ameliorated the oxidative stress and decreased the serum levels of pro-inflammatory cytokines in T2DM model rats. Serum untargeted metabolomics analysis indicated that the EVO treatment affected the levels of 26 metabolites, such as methionine, citric acid, cholesterol, taurocholic acid, pilocarpine, adrenic acid, and other metabolites. These metabolites were mainly related to the amino sugar and nucleotide sugar metabolism, arginine biosynthesis, arginine and proline metabolism, glutathione metabolism, and tryptophan metabolism pathways. In conclusion, EVO can reduce blood glucose and improve oxidative stress and inflammatory response in T2DM rats. These functions are related to the regulation of amino sugar and nucleotide sugar metabolism, arginine biosynthesis, arginine and proline metabolism, glutathione metabolism, and tryptophan metabolism pathways.

Received 19th January 2022,
Accepted 21st April 2022

DOI: 10.1039/d1fo04396j

rsc.li/food-function

Introduction

Type 2 diabetes mellitus (T2DM) is characterized by glucose metabolism disorder and is mainly caused by the inability to produce sufficient insulin in pancreatic β cells or the inability to use insulin effectively.[1] Nowadays, the incidence of T2DM has been gradually increasing, and there are more than 400 million patients with T2DM worldwide.[2] An epidemiology study showed that the global prevalence of diabetes has increased rapidly (from 4.7% to 8.5% population since 1980), which poses a major threat to the well-being of all humans.[3] However, the etiology of T2DM is still not fully understood. The currently used clinical hypoglycemic agents include sulfonylureas, metformin, sitagliptin phosphate, and insulin.[4] However, these treatments do not completely stop the progression of diabetes and can produce many adverse effects, such as hypoglycemia and gastrointestinal discomfort.[5,6]

Natural plants and their active ingredients have more significant advantages in controlling blood glucose and inhibiting inflammatory responses in patients with T2DM.[7,8] Curcumin significantly inhibits the apoptosis of islet β cells and improves their function in rats with T2DM, while reducing insulin resistance.[9] Dioscin improves the disorder of glucose and lipid metabolism in T2DM model rats by promoting STAT3 phosphorylation in hepatocytes.[10] Furthermore, clinical randomized controlled trials have shown that *Momordica charantia* improves overweight and insulin resistance (IR) in patients with T2DM.[11] A meta-analysis found that cinnamon could reduce fasting glucose and improve anthropometric indices in T2DM patients.[12] Therefore, exploring the mechanism of action of natural plants in treating T2DM is proposed to provide an experimental basis for developing novel drugs against T2DM.

[a]*Jiaxing Hospital of Traditional Chinese Medicine, Jiaxing 314001, China. E-mail: cfj1123@sina.com*
[b]*Tianjin University of Traditional Chinese Medicine, Tianjin 301617, China. E-mail: whw2009@tjutcm.edu.cn*
†Yuejie Yu and Qinyan Lu contribute equally to this work.

Evodiamine (EVO) is an alkaloid extracted from *Evodia rutaecarpa* and has various pharmacological activities, including hypolipidemic, anti-inflammatory, anti-infective, and antitumor effects.[13–15] It was previously reported that EVO reduced blood glucose and IR in rats with T2DM.[16] EVO also inhibits adipocyte differentiation *in vitro* and obesity *in vivo*, along with ameliorative effects on IR.[17] However, the specific mechanism by which EVO improves T2DM and insulin resistance has not been studied.

Metabolomics is an effective approach for studying changes in endogenous metabolites, and elucidates the pathogenesis of diseases from metabolic aspect, thereby directly reflecting the current metabolic state of organs or cells.[18] Metabolomics can also identify abnormal metabolic pathways and characteristic biomarkers that are closely associated with diseases, thus providing a basis for further elucidation of disease pathogenesis.[19,20] Nevertheless, many natural plant components can be used to treat T2DM through metabolite regulation. To this end, *Sophora flavescens* extracts were used to treat rats with T2DM through the regulation of lipid metabolism, carbohydrate metabolism and amino acid metabolism.[21] Berberine has also been found to play a role in T2DM treatment by regulating glyoxylate and dicarboxylate metabolism, pentose and glucuronate interconversions and sphingolipid metabolism.[22]

In this study, we used a T2DM rat model using a high-fat diet (HFD) combined with streptozotocin (STZ) injections followed by treatment with EVO. First, we evaluated the therapeutic effects of EVO on T2DM rats, following which we evaluated the anti-inflammatory and anti-oxidative effects of EVO on T2DM rats. Finally, we analyzed the metabolic regulatory mechanism of EVO in T2DM rats using an untargeted metabolomics approach.

Materials and methods

Reagents

EVO ($C_{19}H_{17}N_3O$; molecular weight, 303.36 Da; purity ≥98%; CAS no. 518-17-2) was purchased from Sichuan Weikeqi Biological Technology Co., Ltd (Sichuan, China). HFD, composed of 65.75% of basal chow, 20% of sucrose, 10% of lard, 3% of egg yolk powder, 1% of cholesterol and 0.25% of pig bile salt, was purchased from Beijing Sibeifu Bioscience Co., Ltd (Beijing, China). Streptozotocin (STZ) and metformin were purchased from Solarbio Biotechnology Co., Ltd (Beijing, China). All biochemical test kits (triglyceride (TG), high density lipoprotein (HDL), low density lipoprotein (LDL), total cholesterol (TC), alanine aminotransferase (ALT), aspartate aminotransferase (AST), blood urea nitrogen (BUN), creatinine (Cr), superoxide dismutase (SOD), methane dicarboxylic aldehyde (MDA), and glutathione peroxidase (GSH-Px)) were obtained from Nanjing Jiancheng Biological Engineering Institute (Nanjing, China). Enzyme-linked immunosorbent assay (ELISA) kits of rat insulin, tumor necrosis factor alpha (TNF-α), interleukin (IL)-1β, and IL-6 were purchased from Multi Science Biotechnology Co., Ltd (Hangzhou, China).

Grouping and drug administration method

Fifty specific pathogen free (SPF)-grade male Sprague–Dawley (SD) rats were purchased from Beijing Sibeifu Biotechnology Co, Ltd. The body weights of the rats ranged from180 to 220 g. The housing environment was maintained at 25 °C ± 2 °C, with a 12 h light–dark cycle. All animal experiments were approved by the Animal Ethics Committee at Jiaxing Hospital of Traditional Chinese Medicine.

All rats received adaptive feeding for 1 week. Then, 10 rats were selected randomly as the control group and fed a standard chow, whereas the remaining 40 rats were fed HFD for 8 weeks. After HFD feeding, all rats were fasted for 12 h, followed by receiving intraperitoneal injection of STZ (30 mg kg^{-1}). STZ was dissolved in 0.1 mol L^{-1} citrate buffer (pH = 4.5). Meanwhile, the rats in the control group received intraperitoneal injection of the same volume of citrate buffer. Blood was subsequently collected from their tail veins 72 h after STZ injections to measure their random blood glucose levels, and the model was successfully replicated with blood glucose >16.7 mmol L^{-1}. Subsequently, the groups were divided into T2DM, metformin, EVO low-dose, and EVO high-dose groups randomly (n = 10 per group). Animals in the control and T2DM groups were administered 2 mL of saline, those in the metformin group were administered 0.2 g $(kg\ d)^{-1}$ of metformin, and rats in the EVO low-dose and EVO high-dose groups were treated with 20 mg $(kg\ d)^{-1}$ and 40 mg $(kg\ d)^{-1}$ of EVO, respectively. All drugs were treated orally for 4 weeks. The body weight and fasting blood glucose (FBG) levels were subsequently measured weekly (Fig. 1).

Oral glucose tolerance test (OGTT)

Four weeks after EVO intervention, all rats were fasted without water for 8 h. Their FBG levels were detected and then used as blood glucose levels at 0 min, after which each rat was immediately administered 50% glucose solution (2 g kg^{-1}) through gavage. Subsequent levels of blood glucose were investigated at 30 min, 60 min, 90 min and 120 min after administration of the glucose solution. Then, the blood glucose-time curve was plotted to calculate the area under the curve (AUC) of OGTT.

Serum biochemical indicator test

Four weeks after EVO intervention, the rats were anesthetized after receiving intraperitoneal injection of nembutal (50 mg kg^{-1}). Subsequently, blood was collected and centrifuged at 3000 rpm for 15 min to collect the serum. The serum levels of lipid-related indicators (TG, TC, HDL and LDL), liver function-related indicators (ALT and AST), kidney function-related indicators (Cr and BUN), and oxidative stress-related indicators (SOD, GSH-Px and MDA) were measured in each rat group, following the protocol described in the kit.

ELISA

Four weeks after EVO intervention, serum insulin, IL-1β, IL-6, and TNF-α levels were measured in each group by ELISA, which was performed according to the protocol described in

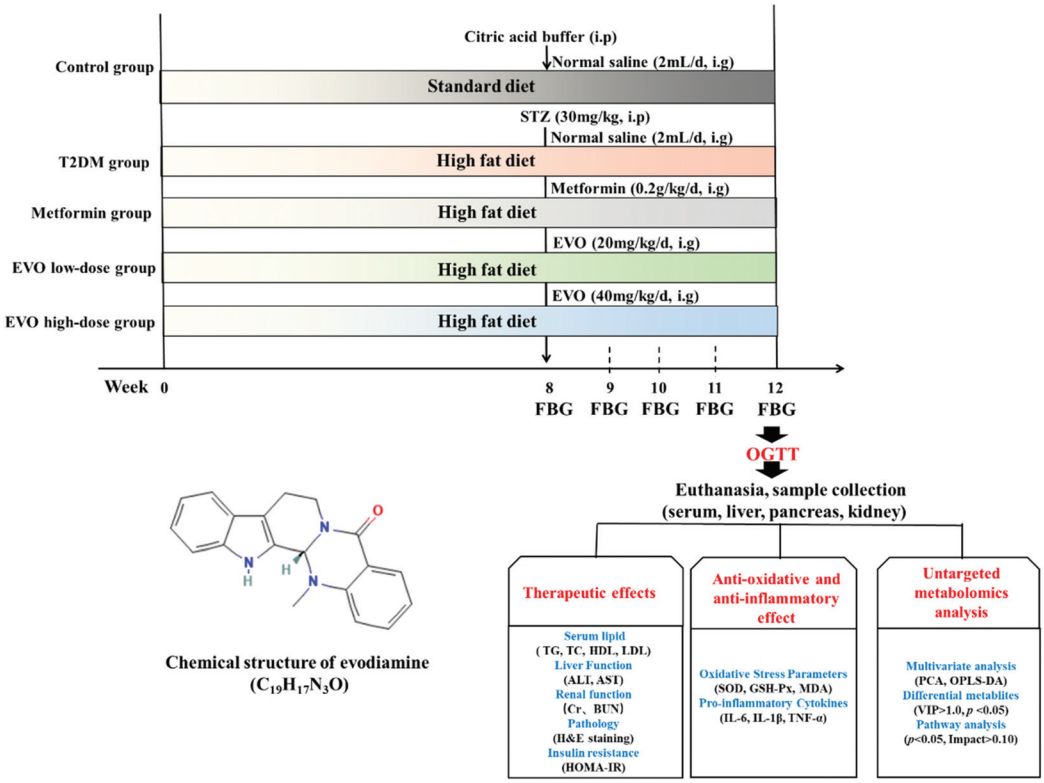

Fig. 1 Overview of the experimental design for all groups.

the kit. Homeostatic model assessment of insulin resistance (HOMA-IR) was then calculated based on the following formula:

$$\text{HOMA-IR} = [\text{FBG (mmol L}^{-1}) \times \text{fasting insulin (FINS, μ IU mL}^{-1})]/22.5$$

Pathology staining

Four weeks after EVO intervention, the liver, pancreas, and kidney tissue samples of rats were fixed in formalin solution, embedded, cut into 3 μm sections, followed by staining with HE. The pathological changes in the liver, pancreas, and kidneys were observed using a light microscope.

Untargeted metabolomics analysis

Serum sample preparation. Briefly, 100 μL of serum sample was added to 400 μL of 80% methanol, vortexed and shaken, placed in an ice bath for 5 min, and then centrifuged for 20 min (15 000*g*, 4 °C). After centrifugation, the supernatant was diluted with ultrapure water to obtain a 53% methanol concentration, followed by centrifugation at 15 000*g* for 20 min at 4 °C. The supernatant was then collected and used as the sample to be tested. All samples were subsequently mixed in equal amounts to be used as the quality control sample (QC). Periodic analysis was performed throughout the analysis process to monitor the stability of the instrument.

Chromatographic and mass spectrometric conditions. Chromatography was performed using a Vanquish UHPLC system (ThermoFisher, Germany) coupled with an Orbitrap Q Exactive™ HF mass spectrometer (Thermo Fisher, Germany). Briefly, the prepared serum samples were injected onto a Hypersil Gold (C_{18}) column (2.1 mm × 100 mm, 1.9 μm, Thermo Fisher, USA) with a mobile phase comprising (A) 0.1% formic acid and (B) methanol, employing the gradient elution method: 0 min, 2% B; 1.5 min, 2% B; 12 min, 100% B; 14 min, 100% B; 14.1 min, 2% B; and 17 min, 2% B. The column temperature was set to 40 °C, the flow rate was 0.2 mL min^{-1}, and the injection volume was 2 μL.

Mass spectrometry was performed with simultaneous detection in positive and negative ion modes using electrospray ionization (ESI), where the settings of the ESI were as follows: aux gas flow rate, 10 arb; sheath gas flow rate, 40 arb; spray voltage, 3.2 kV; and capillary temperature, 320 °C. Throughout the experiment, a QC was added after every six samples to assess the stability of the experiment.

Data processing and analysis

Molecular characteristic peaks of the samples were detected based on the high-resolution mass spectrometry detection technique. The molecular characteristic peaks were matched and identified by combining high-quality mzCloud, mzVault, and MassList databases constructed from the standards. Subsequently, raw files generated from mass spectrometry were analyzed using Compound Discoverer 3.1 (CD 3.1, Thermo Fisher) software for data preprocessing. First, the data were briefly screened based on the retention time and mass-to-

charge ratio, and then the peaks were aligned to enhance the accuracy of identification (retention time deviation of 0.2 min and mass deviation (part per million, ppm) of 5 ppm for different samples). Subsequently, peak extraction and peak area quantification were performed based on the minimum signal intensity of 100 000, settings of 5 ppm, signal-to-noise ratio (S/N) of 3, signal intensity deviation of 30%, and adduct ions. Then, the molecular formula was predicted using molecular ion peaks and fragment ions and compared with mzCloud, mzVault, and MassList databases, from which the metabolites were identified. Metabolites with a coefficient of variance less than 30% (ref. 22) in the QC were retained as the final identification results for subsequent analysis. The peaks detected in the samples were integrated using the CD 3.1 software, wherein the peak area of each characteristic peak represented the relative quantitative value of each metabolite. Furthermore, the quantitative results were normalized using the total peak area. Finally, the quantitative results of the metabolites were obtained. After this, multivariate statistical analysis, including principal component analysis (PCA) and partial least squares discriminant analysis (PLS-DA), was performed to identify the differential metabolites among the different groups. In this, differential biomarkers were screened based on $P \leq 0.05$ and variable importance of projection (VIP) > 1. Metabolic pathway enrichment analysis was conducted for differential metabolites with fold change (FC) > 1.25 or FC < 0.80 based on MetaboAnalyst software and the data obtained from Kyoto Encyclopedia of Genes and Genomes (KEGG).

mzCloud: **https://www.mzcloud.org/**

MetaboAnalyst: **https://www.metaboanalyst.ca/**

Encyclopedia of Genes and Genomes (KEGG): **https://www.kegg.jp/**

Statistical analysis

Statistical analysis was performed using the SPSS 20.0 statistical software. Data were presented as the mean ± standard deviation (SD). One-way analysis of variance was used for comparisons between groups, and differences were considered statistically significant at $P < 0.05$.

Results

Effects of EVO on blood glucose levels, liver and kidney functions, IR, and pathological manifestations in T2DM rats

The body weight was decreased continuously in the T2DM group compared with the control group after STZ injection ($P < 0.01$). In addition, EVO and metformin treatment did not reduce the body weight loss in T2DM model rats (Fig. 2a). FBG levels were >16.7 in rats 72 h after STZ injection, suggesting that the T2DM model was successfully induced. After 4 weeks of EVO intervention, compared with the T2DM group, FBG levels were significantly lower in the metformin, EVO low-dose, and EVO high-dose groups ($P < 0.01$, respectively, Fig. 2b).

In terms of lipid levels, serum TC, TG, and LDL levels were significantly higher and serum HDL levels were significantly lower in the T2DM group than those in the control group ($P < 0.01$, respectively). The levels of TG ($P < 0.01$, respectively) and LDL ($P < 0.01$, respectively) were decreased and the level of HDL ($P < 0.01$, $P < 0.05$ and $P < 0.01$, respectively) was

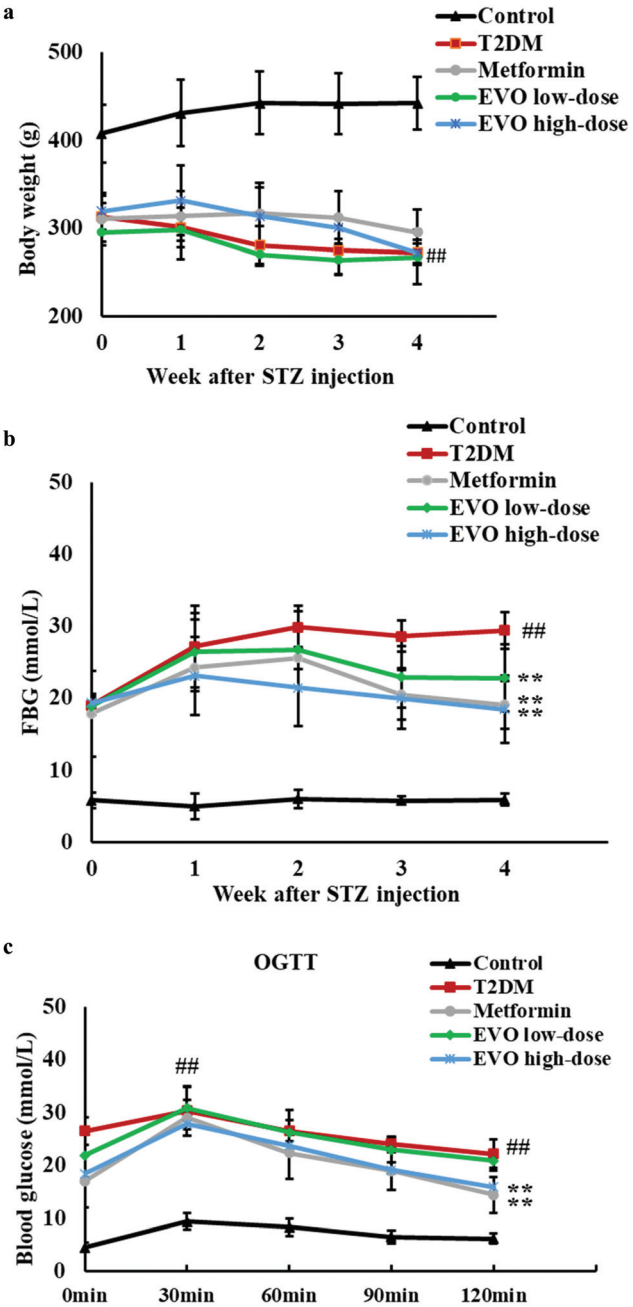

Fig. 2 EVO treatment alleviated the hyperglycemia, hyperlipidemia, IR, and pathological changes in T2DM rats. (a) EVO treatment did not reduce the body weight loss in T2DM model rats. (b) EVO treatment decreased the FBG level in T2DM model rats. (c and d) The AUC of OGTT was decreased in T2DM model rats after EVO treatment. (e) EVO treatment significantly improved the pathological changes of liver, pancreas and kidneys in T2DM model rats (200×). Control, T2DM, metformin, EVO low-dose and EVO high-dose (n = 10 per group) groups. ##: $P < 0.01$ compared with the control group; **: $P < 0.01$ compared with the T2DM group.

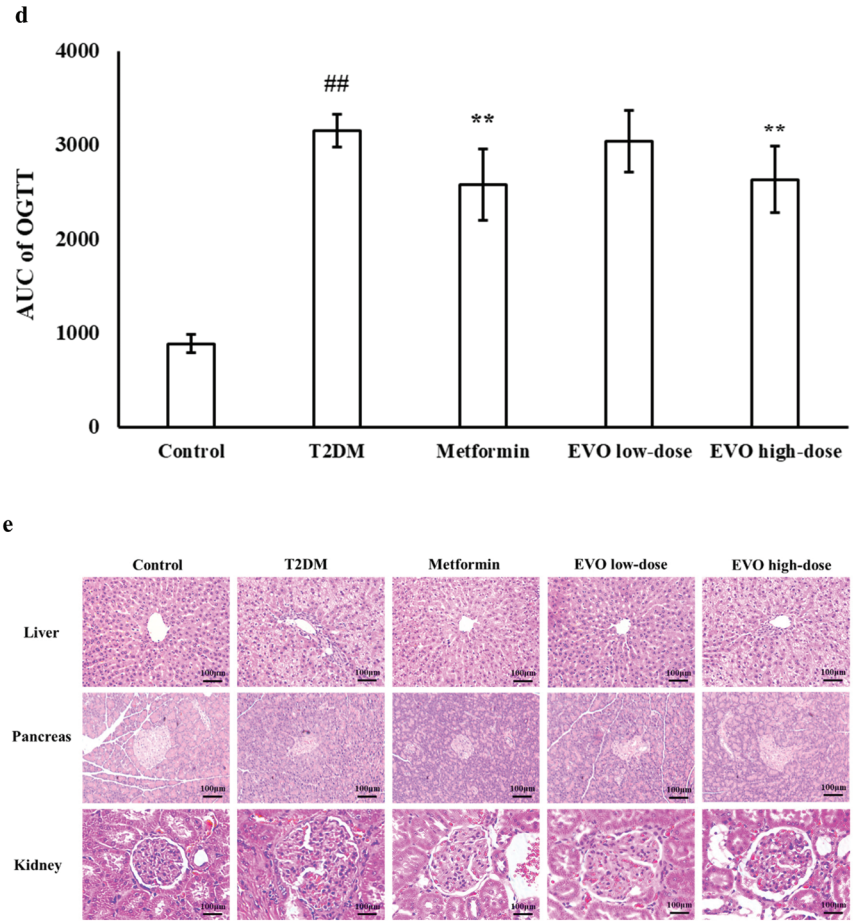

Fig. 2 *(Contd)*.

increased in metformin, EVO low-dose and EVO high-dose groups compared with the T2DM group. The level of TC was decreased in metformin ($P < 0.01$) and EVO high-dose ($P < 0.05$) groups compared with the T2DM group (Table 1). Liver and kidney function tests showed that the serum levels of ALT, AST, Cr, and BUN were significantly increased in the T2DM group than those in the control group ($P < 0.01$, respectively). Moreover, the interventions of metformin and high-dose EVO significantly decreased the serum activities of AST ($P < 0.01$ and $P < 0.05$, respectively), ALT ($P < 0.01$ and $P < 0.05$, respectively) and serum levels of Cr ($P < 0.01$ and $P < 0.05$, respectively) and BUN ($P < 0.01$, respectively) in T2DM rats (Table 2). The OGTT results showed that the OGTT-AUC of rats in the T2DM group was significantly increased compared with that of rats in the control group ($P < 0.01$), whereas it was significantly decreased following the interventions of metformin and high-dose EVO ($P < 0.01$, respectively, Fig. 2c and d). Furthermore, compared with the control group, the FINS level ($P < 0.01$) and HOMA-IR ($P < 0.01$) in T2DM rats were significantly increased, whereas treatment of metformin and high-dose EVO signifi-

Table 1 Changes in blood lipid levels after EVO treatment

Group	TC (mmol L^{-1})	TG (mmol L^{-1})	HDL (mmol L^{-1})	LDL (mmol L^{-1})
Control	13.01 ± 4.65	2.07 ± 0.61	11.46 ± 4.14	2.79 ± 0.26
T2DM	31.74 ± 7.59$^{\#\#}$	5.98 ± 0.22$^{\#\#}$	4.92 ± 2.00$^{\#\#}$	4.93 ± 0.42$^{\#\#}$
Metformin	20.03 ± 4.13**	2.12 ± 0.20**	8.61 ± 1.79**	3.39 ± 0.82**
EVO low-dose	26.17 ± 6.10	4.87 ± 0.89**	6.66 ± 1.38*	3.90 ± 0.46**
EVO high-dose	24.20 ± 5.48*	3.25 ± 0.51**	9.18 ± 1.52**	3.72 ± 0.48**

Control, T2DM, metformin, EVO low-dose and EVO high-dose ($n = 10$ per group) groups. $^{\#\#}$: $P < 0.01$ compared with the control group; *: $P < 0.05$ compared with the T2DM group; **: $P < 0.01$ compared with the T2DM group.

Table 2 Changes in serum AST and ALT activities and serum Cr and BUN levels after EVO treatment

Group	AST (U L^{-1})	ALT (U L^{-1})	Cr (μmol L^{-1})	BUN (mmol L^{-1})
Control	94.3 ± 20.71	34.54 ± 18.84	59.54 ± 11.79	3.68 ± 0.58
T2DM	206.21 ± 80.00##	80.57 ± 25.68##	110.60 ± 23.16##	9.60 ± 1.21##
Metformin	102.74 ± 34.01**	44.76 ± 22.88**	78.85 ± 15.69**	5.41 ± 0.86**
EVO low-dose	162.85 ± 70.67	64.73 ± 14.71	98.38 ± 11.89	8.79 ± 0.57
EVO high-dose	134.91 ± 62.81*	53.97 ± 29.35*	83.17 ± 24.19*	5.77 ± 0.70**

Control, T2DM, metformin, EVO low-dose and EVO high-dose (n = 10 per group) groups. ##: $P < 0.01$ compared with the control group; *: $P < 0.05$ compared with the T2DM group; **: $P < 0.01$ compared with the T2DM group.

Table 3 Levels of FINS and HOMA-IR after EVO treatment

Group	FINS (μ IU ml^{-1})	HOMA-IR
Control	6.33 ± 1.60	1.68 ± 0.53
T2DM	10.72 ± 2.48##	14.12 ± 4.02##
Metformin	6.95 ± 1.73**	5.85 ± 1.65**
EVO low-dose	9.19 ± 6.54	10.42 ± 2.46*
EVO high-dose	8.44 ± 1.99*	6.67 ± 0.91**

Control, T2DM, metformin, EVO low-dose and EVO high-dose (n = 10 per group) groups. ##: $P < 0.01$ compared with the control group; *: $P < 0.05$ compared with the T2DM group; **: $P < 0.01$ compared with the T2DM group.

Table 4 Changes in serum SOD and GSH-Px activities and the serum MDA level after EVO treatment

Group	SOD (U mL^{-1})	MDA (nmol mL^{-1})	GSH-Px (μmol L^{-1})
Control	174.29 ± 34.57	4.51 ± 0.86	104.65 ± 21.05
T2DM	98.14 ± 30.56##	20.18 ± 3.19##	66.22 ± 19.36##
Metformin	131.43 ± 21.41*	14.27 ± 2.75**	90.32 ± 21.04*
EVO low-dose	105.62 ± 21.78	18.28 ± 1.85	71.08 ± 25.55
EVO high-dose	129.70 ± 32.09**	14.34 ± 1.58**	84.97 ± 14.21*

Control, T2DM, metformin, EVO low-dose and EVO high-dose (n = 10 per group) groups. ##: $P < 0.01$ compared with the control group; *: $P < 0.05$ compared with the T2DM group; **: $P < 0.01$ compared with the T2DM group.

cantly decreased the FINS level in T2DM rats ($P < 0.01$ and $P < 0.05$, respectively). The HOMA-IR was lower in metformin, EVO low-dose and EVO high-dose groups compared with the T2DM group ($P < 0.01$, $P < 0.05$ and $P < 0.01$, respectively, Table 3).

The results of HE staining of the liver showed that the liver of T2DM rats demonstrated evident hepatocyte steatosis, with some hepatocytes showing necrosis and inflammatory cell infiltration. Moreover, the pancreas showed pancreatic islet atrophy and islet cell damage, whereas the kidneys showed glomerular basement membrane hyperplasia, renal tubular atrophy, and extensive inflammatory cell infiltration. Metformin and high-dose EVO interventions significantly improved these pathological changes in the liver, pancreatic islets, and kidneys of T2DM rats (Fig. 2e).

Effects of EVO on oxidative stress levels and inflammatory factors in T2DM rats

We evaluated the effects of EVO bases on oxidative stress in T2DM rats by further measuring SOD and GSH-Px activities and MDA levels in the serum of rats from each group. Compared to the control group, SOD and GSH-Px activities in the serum were significantly lower, whereas the MDA levels were significantly higher in T2DM rats ($P < 0.01$, respectively). The interventions of metformin, and high-dose EVO significantly increased SOD ($P < 0.05$ and $P < 0.01$, respectively) and GSH-Px ($P < 0.01$, respectively) activities and decreased MDA ($P < 0.05$, respectively) levels in the serum of T2DM rats (Table 4).

Additionally, this study used ELISA to detect the levels of proinflammatory factors (IL-6, IL-1β, and TNF-α) in the serum of rats from each group to assess the effects of EVO on inflammatory responses in T2DM rats. The results showed that the serum levels of IL-6, IL-1β, and TNF-α were significantly higher in T2DM rats than those in the control group ($P < 0.01$, respectively). Moreover, the interventions of metformin, low-dose EVO, and high-dose EVO significantly reduced the serum level of IL-6 in T2DM rats ($P < 0.01$, respectively). The levels of IL-1β and TNF-α were lower in metformin and EVO low-dose groups compared with those in the T2DM group ($P < 0.01$, respectively, Fig. 3). The above results indicated that high-dose EVO showed significant efficacy in treating T2DM. As a result, the EVO high-dose group was selected for subsequent untargeted metabolomic tests.

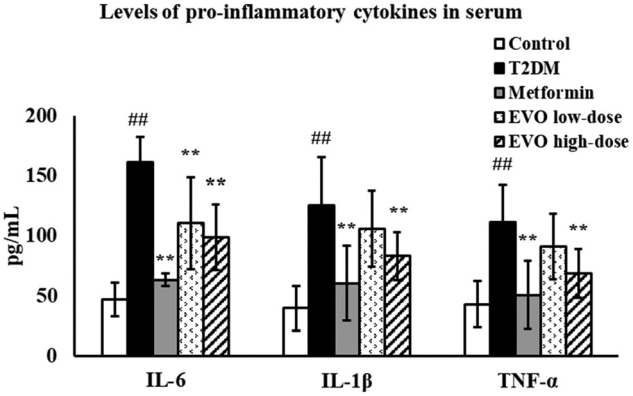

Fig. 3 EVO treatment decreased the serum levels of pro-inflammatory cytokines (IL-6, IL-1β, and TNF-α) in T2DM model rats. Control, T2DM, metformin, EVO low-dose and EVO high-dose (n = 10 per group) groups. ##: $P < 0.01$ compared with the control group; **: $P < 0.01$ compared with the T2DM group.

Effects of EVO on serum metabolite levels in T2DM rats

The PCA plots showed that the control group was well distinguished from the T2DM group and the T2DM group was well distinguished from the EVO high-dose group (Fig. 4a). To identify the differential metabolites, the PLS-DA model was used, and the coefficient of determination (R^2) and predictive power (Q^2) of the model were evaluated. These values were as follows when the T2DM group was compared with the control group: R^2 = 0.86 and Q^2 = −0.84. Similarly, the values were as follows when the EVO high-dose group was compared with the T2DM group: R^2 = 0.88 and Q^2 = −0.86 (Fig. 4b–e). These results indicated that the model was stable and had good predictive ability.

The following two criteria were used to screen differential metabolites: $P < 0.05$ and VIP > 1.0. As a result, 26 differential metabolites were identified (Table 5). Compared with the control group, in the serum of rats in the T2DM group, the levels of methionine, fumaric acid, *N*-acetyl-D-glucosamine, citric acid, cholesterol, D-(+)-maltose, L-kynurenine, glycocholic acid, 13-HPODE, taurocholic acid, taurochenodeoxycholic acid, and erucic acid were significantly elevated, whereas the levels of glutathione, ornithine, shikimic acid, 3-hydroxyanthranilic acid, L-fucose, melatonin, acetylcholine, nervonic acid, kahweol, docosapentaenoic acid, and cholesteryl sulfate were significantly decreased. Furthermore, compared with the T2DM group, the levels of glutathione, ornithine, shikimic acid, 3-hydroxyanthranilic acid, L-fucose, melatonin, acetylcholine, genistein, nervonic acid, and kahweol were significantly higher, whereas the levels of methionine, fumaric acid, *N*-acetyl-D-glucosamine, citric acid, cholesterol, L-kynurenine, glycocholic acid, taurocholic acid, taurochenodeoxycholic acid, pilocarpine, and adrenic acid were significantly reduced in EVO high-dose group.

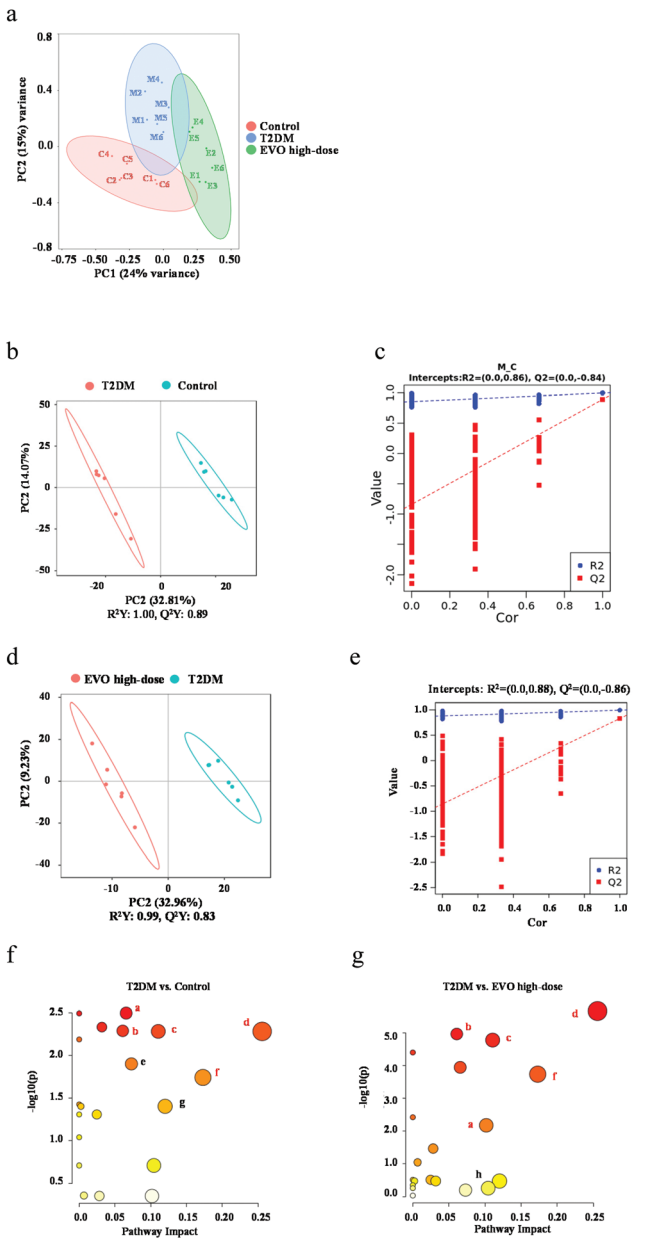

Fig. 4 Multivariate statistical analysis and pathway analysis of serum untargeted metabolomics. (a) Score plots of PCA among the control, T2DM and EVO high-dose groups. (b–e) Score plots of PLS-DA (b and d) and the coefficient of loading plots (c and e). (f and g) Summary of pathway analysis of serum samples between control and T2DM groups (f) and between T2DM and EVO high-dose groups (g). a: Amino sugar and nucleotide sugar metabolism; b: arginine biosynthesis; c: arginine and proline metabolism; d: glutathione metabolism; e: starch and sucrose metabolism; f: tryptophan metabolism; g: citrate cycle (TCA cycle); and h: primary bile acid biosynthesis. Control, T2DM, EVO high-dose (n = 6 per group) groups.

Analysis of differential metabolic pathways in the serum after EVO intervention in T2DM rats

MetaboAnalyst was used to perform the enrichment analysis of metabolic pathways for differential metabolites in T2DM rats, and KEGG was selected as the database to screen differential metabolic pathways based on the conditions of pathway impact >0.1 and $P < 0.05$. The differential metabolic pathways between the control and T2DM groups included amino sugar and nucleotide sugar metabolism, arginine biosynthesis, arginine and proline metabolism, glutathione metabolism, starch and sucrose metabolism, tryptophan metabolism, and the citrate cycle (TCA cycle) (Fig. 4f). The differential metabolic pathways between the T2DM and EVO high-dose groups included amino sugar and nucleotide sugar metabolism, arginine biosynthesis, arginine and proline metabolism, glutathione metabolism, tryptophan metabolism, and primary bile acid biosynthesis (Fig. 4g). Among them, amino sugar and nucleotide sugar metabolism, arginine biosynthesis, arginine and proline metabolism, glutathione metabolism, and tryptophan metabolism pathways were the common pathways between the normal and T2DM groups and between the T2DM and EVO high-dose groups. These pathways were therefore selected as the metabolic pathways for EVO intervention in treating T2DM. Hence, these pathways were discussed in detail.

Table 5 The differential metabolites in serum after EVO treatment

Formula	RT [min]	*m/z*	Metabolites	VIP		FC		Trend		Pathway
				T vs. C	*E vs. T*	*T vs. C*	*E vs. T*	*T vs. C*	*E vs. T*	
$C_{10}H_{17}N_3O_6S$	10.76	308.09	Glutathione	1.49	1.04	0.61	1.31	↓**	↑**	d
$C_5H_{11}NO_2S$	1.43	150.06	Methionine	1.33	1.96	1.47	0.74	↑*	↓*	
$C_5H_{12}N_2O_2$	1.14	133.10	Ornithine	1.62	1.32	0.30	3.03	↓**	↑**	b,d
$C_4H_4O_4$	1.20	115.00	Fumaric acid	1.11	1.60	1.64	0.67	↑**	↓**	b,c,g
$C_8H_{15}NO_6$	12.68	220.08	*N*-Acetyl-D-glucosamine	1.35	2.04	1.60	0.65	↑**	↓**	a
$C_6H_8O_7$	6.00	191.02	Citric acid	1.34	1.73	1.78	0.64	↑**	↓*	g
$C_{27}H_{46}O$	15.23	387.36	Cholesterol	1.70	1.98	1.39	0.65	↑*	↓**	h
$C_{12}H_{22}O_{11}$	1.34	365.11	D-(+)-Maltose	1.31	2.26	1.78	0.71	↑**	↓	e
$C_{10}H_{12}N_2O_3$	8.39	209.09	L-Kynurenine	1.32	1.61	1.64	0.68	↑*	↓**	f
$C_7H_{10}O_5$	9.33	233.07	Shikimic acid	1.39	1.05	0.13	3.97	↓**	↑**	
$C_7H_7NO_3$	3.31	154.05	3-Hydroxyanthranilic acid	1.97	1.28	0.32	1.72	↓**	↑*	f
$C_6H_{12}O_5$	1.35	163.06	L-Fucose	1.28	1.13	0.50	1.80	↓**	↑**	a
$C_{13}H_{16}N_2O_2$	8.77	231.11	Melatonin	1.92	1.06	0.59	1.52	↓**	↑**	f
$C_{26}H_{43}NO_6$	11.15	464.30	Glycocholic acid	1.88	1.38	1.67	0.54	↑**	↓**	h
$C_7H_{15}NO_2$	1.36	146.12	Acetylcholine	1.34	1.99	0.63	1.34	↓**	↑*	
$C_{18}H_{32}O_4$	13.06	313.24	13-HPODE	1.23	1.69	1.69	0.81	↑**	↓	
$C_{26}H_{45}NO_7S$	12.46	514.28	Taurocholic acid	1.56	1.26	1.90	0.69	↑*	↓*	h
$C_{26}H_{45}NO_6S$	12.73	498.29	Taurochenodeoxycholic acid	1.62	1.97	1.82	0.53	↑**	↓**	h
$C_{15}H_{10}O_5$	10.71	269.05	Genistein	1.24	2.02	0.79	1.42	↓	↑*	
$C_{11}H_{16}N_2O_2$	9.04	209.13	Pilocarpine	1.92	2.33	1.27	0.55	↑	↓*	
$C_{22}H_{42}O_2$	15.20	337.31	Erucic acid	1.98	2.08	1.67	0.79	↑*	↓	
$C_{24}H_{46}O_2$	15.58	365.34	Nervonic acid	2.16	1.97	0.57	1.79	↓**	↑*	
$C_{20}H_{26}O_3$	13.07	315.20	Kahweol	2.08	1.45	0.31	2.46	↓**	↑*	
$C_{22}H_{34}O_2$	15.21	331.26	Docosapentaenoic acid	1.25	1.09	0.49	2.94	↓**	↑	
$C_{22}H_{36}O_2$	14.55	331.26	Adrenic acid	1.66	1.11	1.68	0.61	↑	↓*	
$C_{27}H_{46}O_4S$	12.13	465.30	Cholesteryl sulfate	2.09	1.14	0.57	1.20	↓*	↑	

Control, T2DM, EVO high-dose (n = 6 per group) groups. *, $p < 0.05$; **, $p < 0.01$; ↑, increased; ↓, decreased; *vs.*, *versus*; C, control group; T, T2DM; E, EVO high-dose group. a: Amino sugar and nucleotide sugar metabolism; b: arginine biosynthesis; c: arginine and proline metabolism; d: glutathione metabolism; e: starch and sucrose metabolism; f: tryptophan metabolism; g: citrate cycle (TCA cycle); and h: primary bile acid biosynthesis.

Discussion

In this study, T2DM was induced in rats using a HFD combined with STZ injections, which is consistent with our previous study.[23] Our results showed that compared to the control group, rats in the T2DM group had significantly higher FBG levels. However, the results of serum biochemical indicators suggested that the rats in the T2DM group exhibited dyslipidemia. The elevation observed in ALT, AST, Cr, and BUN levels also suggested that the rats in the T2DM group had abnormal liver and kidney functions. Moreover, the AUC and HOMA-IR of OGTT in the rats of the T2DM group were elevated, suggesting IR. Furthermore, pathological results showed evident hepatic steatosis in the rats of the T2DM group, as hepatocytes showed vacuolated and ballooned changes and were enlarged and disorganized. Moreover, the pancreatic tissue showed evident atrophy of pancreatic islets, with islet cell damage, and an evident reduction in the number of islet cells, which were sparsely distributed. Vacuolated changes were also observed, with the renal tissue showing swollen glomeruli, enlarged volume, swollen or detached tubular epithelial cells, hyperplasia of some mesangial matrices, and interstitial fibrosis. The above results are consistent with the expected pathological manifestations of T2DM.[24,25] The administration of EVO reduced blood glucose levels and improved dyslipidemia, IR, and pathological changes in the liver, pancreas, and kidney tissues of T2DM rats, with more significant effects being observed in the high-dose group, suggesting that EVO has a therapeutic effect on T2DM. Additionally, metformin was selected as a positive control for treating T2DM in this study.[26] Metformin is a clinical drug used for the treatment of T2DM.[27] The results showed no significant differences in the improvement of blood glucose levels, IR, and liver and kidney functions between the rats in the EVO high-dose and metformin groups, which suggested that EVO has the potential to be an alternative therapy to metformin for the treatment of T2DM.

Oxidative stress is closely related to the development of T2DM.[28] T2DM presents with glucose and lipid metabolism disorder, where hyperglycemia and hyperlipidemia lead to the production of large amounts of reactive oxygen species (ROS) in the mitochondria, thereby disrupting mitochondrial function and causing oxidative stress.[29] Oxidative stress then leads to IR and induces the development of T2DM by inhibiting insulin secretion, promoting β-cell apoptosis, decreasing insulin gene expression, and blocking insulin action pathways.[30–32] Our results revealed that EVO increased the activities of antioxidant enzymes SOD and GSH-Px and decreased the levels of MDA in the serum of T2DM rats. It has been reported that SOD and GSH-Px are antioxidant enzymes

that respond to the strength of antioxidant capacity.[33] SOD acts as an intracellular oxygen radical scavenger, catalyzing the conversion of O_2^- to O_2 and H_2O_2, thereby protecting the organism from superoxide anions.[34] GSH-Px is an important peroxide-degrading enzyme that is widely present in the body. It catalyzes the conversion of reduced glutathione (L-glutathione, GSH) to its oxidized form (glutathione disulfide, GSSG) and protects cells from peroxide-induced disruption and damage.[35] Oxidative stress leads to the production of large amounts of free radicals, which cause lipid peroxidation and consequently cellular damage.[36] MDA is a product of lipid peroxidation caused by free radicals or ROS in cells under oxidative stress, and MDA levels can indirectly reflect the degree of oxidative damage in cells.[37]

Local and systemic proinflammatory cytokines, such as IL-6, IL-1β, and TNF-α, are key triggers of the inflammatory microenvironment of pancreatic islets. The production of proinflammatory factors exacerbates the induction of IR, whereas metabolic stress during T2DM stimulates islet cells to produce more inflammatory factors, leading to a vicious cycle of T2DM.[38] Our experimental results showed that EVO reduced the levels of serum proinflammatory factors IL-6, IL-1β, and TNF-α in T2DM rats. IL-6 is a multifunctional cytokine that reduces insulin activity by interfering with insulin receptor signaling and impairing β-cell functions, leading to the development of IR. In the process, it inhibits the synthesis of glycogen and promotes the development of T2DM by inhibiting the activity of components in the downstream parts of the insulin receptor signaling pathway.[39] IL-1β is the main proinflammatory factor that mediates islet β-cell damage and leads to abnormal insulin secretion in T2DM. Intercellular adhesion molecule-1 (ICAM-1) is responsible for islet β-cell damage and death, and IL-1β contributes to increased ICAM-1 secretion, further exacerbating the severity of diabetes.[40] Moreover, TNF-α increases β-cell apoptosis and reduces glucose-stimulated insulin secretion (GSIS),[41] thereby affecting normal glucose metabolism.

We investigated the effect of EVO on the serum metabolites of T2DM rats using untargeted metabolomics. PCA and PLS-DA analysis results revealed significant changes in serum metabolism in T2DM rats. Furthermore, EVO administration significantly affected serum metabolism levels in T2DM rats. The results of differential metabolite analysis showed that EVO affected the levels of 26 metabolites, including methionine, citric acid, cholesterol, and D-(+)-maltose. EVO administration reduced the levels of methionine, citric acid, cholesterol, taurocholic acid, pilocarpine, adrenic acid, and other metabolites. An abnormal methionine metabolic cycle was closely associated with the development of diabetic vasculopathy. A previous study reported that compared to normal rats, the conversion of *S*-adenosyl-L-homocysteine to methionine was increased in Zucker diabetic fatty rats, whereas the catabolism of methionine was decreased in these rats. This accumulation of methionine in the serum was involved in the pathogenesis of T2DM, and the addition of methionine to the food of rats exacerbated the metabolic disorder in Zucker diabetic fatty rats.[42] Citric acid is an important intermediate in the TCA cycle and an important substrate for cellular energy metabolism. Citric acid levels are significantly elevated in patients with T2DM and are closely associated with pathological processes, such as T2DM, inflammation, insulin resistance, and metabolic disorders.[43] Excessive intake of nutrients in patients with T2DM can therefore lead to hyperlipidemia, glucose and lipid metabolism disorders, and elevated cholesterol levels, which in turn aggravate several pathological processes, such as IR. Taurocholic acid is an endogenous bile acid, and some studies claim that it has certain antidiabetic effects. In T2DM rats, taurocholic acid levels were significantly increased, and the administration of taurocholic acid did not exert any hypoglycemic effect.[44] Therefore, the relationship between taurocholic acid and T2DM requires further investigation. Additionally, the specific mechanism by which EVO reduces taurocholic acid levels and improves T2DM also requires further elucidation. The relationship between pilocarpine and T2DM has not been reported yet. However, pilocarpine can induce oxidative stress in the nervous system.[43] Docosapentaenoic acid is a metabolite of arachidonic acid, which is significantly increased in patients with nonalcoholic fatty liver diseases (NAFLD). It is a long-chain ω-3 polyunsaturated fatty acid that has anti-inflammatory, hypolipidemic, and immunomodulatory effects.[45,46] Studies have also shown that the administration of docosapentaenoic acid increases ROS levels and induces oxidative stress injury in hepatocytes. Hence, the EVO-dependent inhibition oxidative stress is proposed to be related to the reduction of pilocarpine and docosapentaenoic acid. Our results also found that EVO can increase the levels of nervonic acid, docosapentaenoic acid, and cholesteryl sulfate in the serum of rats with T2DM. The addition of nervonic acid to food can significantly reduce the body weight and lipid metabolism disorders in obese mice and promote the β-oxidation of fatty acids.[47] Cholesteryl sulfate can inhibit ROS production, thereby improving oxidative stress in neuronal cells through the AKT pathway.[48] However, the relationship between cholesteryl sulfate and T2DM has not been reported yet. Therefore, the possibility that EVO can exert antioxidant effects through an increase in cholesteryl sulfate is proposed to be a direction for future research.

Metabolic pathway analysis of the differential metabolites using MetaboAnalyst showed that amino sugar and nucleotide sugar metabolism, arginine biosynthesis, arginine and proline metabolism, glutathione metabolism, and tryptophan metabolism pathways were altered in the control, T2DM, and EVO high-dose groups, suggesting that EVO exerts its therapeutic effect on T2DM by regulating the abovementioned pathways.

Amino sugar and nucleotide sugar metabolism

Amino sugar and nucleotide sugar metabolism is closely related to T2DM.[49] In our study, we observed that although the level of *N*-acetyl-D-glucosamine was elevated in T2DM rats, it was significantly decreased after EVO administration. The results also showed that the decreased levels of L-fucose were significantly increased after EVO administration. As reported

previously, *N*-acetyl-D-glucosamine is a form of glycosylation,[50] by which oligosaccharides are covalently bound to specific amino acid residues on proteins in the form of glycosides.[51] Abnormalities in glycosylation are therefore closely associated with T2DM, where excessive glycosylation of some proteins in the insulin signaling pathway results in decreased phosphorylation, ultimately increasing the flow through the gluconeogenic pathway and decreasing the synthesis of glycogen. All these processes consequently result in glucose tolerance.[52] L-Fucose is a six-carbon sugar and one of the eight essential sugars in the body. It has various pharmacological effects, including anti-inflammatory, anti-infective immune-enhancing effects, and helps in maintaining the balance of beneficial gut microbiota.[53–55] L-Fucose can also reduce colitis by inhibiting the polarization of macrophage M1, inhibiting NLRP3 inflammasomes and NF-κB activation, and downregulating proinflammatory cytokines.[53] Moreover, L-fucose is closely associated with metabolic diseases as it activates the AMPK signaling pathway to enhance insulin sensitivity and stimulate fatty acid oxidation.[56] L-Fucose could also enhance glucose metabolism and lipid metabolism and improve HFD-induced obesity.[57]

Arginine biosynthesis and arginine and proline metabolism

Amino acid metabolism is closely related to the metabolic disorders of diabetes. In our study, we found that fumaric acid levels were elevated in T2DM rats. These levels were significantly reduced after EVO administration. Conversely, the reduced levels of ornithine were significantly increased after EVO administration. Arginine metabolism is closely related to T2DM, and the ratio of arginine to ornithine is also positively associated with the risk of T2DM.[58] Arginine is the largest nitrogen-donating amino acid in the body and is a precursor of proline and creatine.[59] Therefore, arginine metabolism plays a key role in various metabolic processes, including the urea cycle, amino acid and creatine synthesis, immune function regulation, and NO synthesis.[60,61] Fumaric acid is a dicarboxylic acid involved in the TCA cycle. Succinate dehydrogenase catalyzes the production of fumaric acid from its precursor, adenosine, after which fumarase hydratase catalyzes its conversion to malic acid.[62] Disorders of fumaric acid metabolism are proposed to be associated with renal function impairment in diabetes, and the accumulation of fumaric acid leads to oxidative stress.[63] Moreover, ongoing oxidative stress leads to renal injury in diabetes. One study found that the accumulation of fumaric acid was positively correlated with progression toward diabetic nephropathy in patients with T2DM.[64] Furthermore, elevated levels of fumaric acid in patients with diabetes can stimulate endoplasmic reticulum stress and HIF-1α expression, thereby driving the metabolic flow to the glycolytic pathway, which leads to renal pathological injury.[65–67] Ornithine is synthesized from L-arginine in the liver and is produced as an intermediate molecule in the urea cycle. It participates in the regulation of several metabolic processes.[68] It has been reported that the level of serum ornithine is negatively correlated with inflammation.[69] The levels of plasma ornithine were previously observed to be significantly lower in patients with T2DM than in healthy subjects.[70] In the urea cycle, ornithine reduces excess nitrogen by converting ammonia to urea, thereby avoiding the development of hyperammonemia.[71]

Glutathione metabolism

The pathogenesis of T2DM is complex, and studies have shown that oxidative stress plays an important role in its occurrence and development.[72,73] In our study, we found that the levels of GSH were reduced in T2DM rats, which significantly increased after EVO administration. GSH is an important member of the antioxidant defense system of the body and contributes to the scavenging of free radicals, thereby reducing oxidative damage. Some studies have found that the levels of GSH were reduced in patients with T2DM, which is consistent with our experimental results.[74–77] High blood glucose levels can increase the production of ROS through various pathways, and the autoxidation of glucose can lead to the formation of reduced oxidation products, which can damage lipids and proteins and accelerate the formation of glycosylation end-products (AGEs), consequently contributing to the production of more free radicals and leading to tissue injury.[78] High blood glucose levels also increase NADH/NAD^+ levels in the cytoplasm, which decreases GSH levels by interfering with NADH/NAD^+ homeostasis through glycolysis. This increases the susceptibility of endothelial cells to H_2O_2-induced damage.[79] Furthermore, it has been shown that glutathione is involved in glucose-induced insulin secretion, and the ratio of GSH to glutathione disulfide (GSSG) reflects cellular redox homeostasis. In a diabetic rat model, the GSH/GSSG ratio was reduced, indicating an impaired renal glutathione defense system.[80] The GSH/GSSG ratio in the plasma affects cellular responsiveness to glucose, and an increase in the ratio improves the action of peripheral insulin, reduces the extent of oxidative damage, and increases insulin sensitivity in patients with diabetes.[81]

Tryptophan metabolism

Tryptophan metabolism is closely related to chronic inflammatory responses,[82] including oxidative damage[83] and glycolipid metabolism.[84] Our study showed that EVO reduced the level of L-kynurenine, a product related to tryptophan metabolism, in the serum of T2DM rats. Indoleamine-2,3-dioxygenase 1 (IDO1) catalyzes the conversion of tryptophan to L-kynurenine. In the STZ-induced diabetic rat model, the tryptophan metabolism-related products, L-kynurenine, L-kynurenic acid, quinolinic acid, and picolinic acid, were significantly elevated, and the accumulation of these metabolites was involved in the processes of insulin resistance and chronic inflammatory response in diabetes.[85] EVO can also increase the levels of 3-hydroxyanthranilic acid and melatonin, which are also tryptophan metabolism-related products. Many studies have shown that 3-hydroxyanthranilic acid has anti-inflammatory effects and alleviates asthma by inhibiting PDK1 activation and thus inhibiting T-cell activation in an asthma model.[86] In addition, 3-hydroxyanthranilic acid inhibits LPS-induced microglial activation through the upregulation of HO–1

expression, which in turn suppresses neuroinflammatory responses.[87] The antioxidant effects of melatonin have been reported in many studies, where it was reported to inhibit free radical production in the body by regulating electron transfer and hydrogen transfer.[88] Melatonin can also inhibit ROS production in the mitochondria by regulating the exchange of Na^+ and Ca^{2+} in mitochondrial membranes, thereby protecting cells from oxidative damage.[88] Recently, numerous studies have shown that gut microbiota can influence glucose and lipid metabolism and participate in the progression of metabolic diseases, such as obesity, T2DM, and NAFLD, through tryptophan metabolism.[89] Therefore, future research should investigate whether EVO can influence tryptophan metabolism by regulating gut microbiota for treating T2DM.

Conclusion

In conclusion, EVO can reduce blood glucose and improve oxidative stress and inflammatory response in T2DM rats. These functions are related to the regulation of amino sugar and nucleotide sugar metabolism, arginine biosynthesis, arginine and proline metabolism, glutathione metabolism, and tryptophan metabolism pathways.

Ethical statement

All animal procedures were performed in accordance with the Guidelines for Care and Use of Laboratory Animals of Tianjin University of Traditional Chinese Medicine and approved by the Animal Ethics Committee of Tianjin University of Traditional Chinese Medicine.

Conflicts of interest

The authors declare no conflict of interest.

Acknowledgements

This work was supported by the National Science Foundation of China (No. 82104802) and the Scientific research Project of Tianjin Education Commission (2021ZD010).

References

1 F. khatami, M. R. Mohajeri-Tehrani and S. M. Tavangar, *Endocr., Metab. Immune Disord.: Drug Targets*, 2019, **19**(6), 719–731.
2 C. Zhu, W. Zhang, J. Liu, B. Mu, F. Zhang, N. Lai, J. Zhou, A. Xu and Y. Li, *Mol. Med. Rep.*, 2017, **16**, 3947–3957.
3 M. J. Davies, K. Merton, U. Vijapurkar, J. Yee and R. Qiu, *Cardiovasc. Diabetol.*, 2017, **16**(1), 40.
4 R. A. DeFronzo, *Ann. Intern. Med.*, 2000, **133**, 73.
5 M. O. Goodarzi and M. Bryer-Ash, *Diabetes, Obes. Metab.*, 2005, **7**, 654–665.
6 P. D. Home, S. J. Pocock, H. Beck-Nielsen, P. S. Curtis, R. Gomis, M. Hanefeld, N. P. Jones, M. Komajda and J. J. McMurray, *Lancet*, 2009, **373**, 2125–2135.
7 J. Ríos, F. Francini and G. Schinella, *Planta Med.*, 2015, **81**, 975–994.
8 W. Li, H. Zheng, J. Bukuru and N. D. Kimpe, *J. Ethnopharmacol.*, 2004, **92**, 1–21.
9 F. Pivari, A. Mingione, C. Brasacchio and L. Soldati, *Nutrients*, 2019, **11**, 1837.
10 L.-N. Xu, L.-H. Yin, Y. Jin, Y. Qi, X. Han, Y.-W. Xu, K.-X. Liu, Y.-Y. Zhao and J.-Y. Peng, *Phytomedicine*, 2020, **67**, 153139.
11 M. Cortez-Navarrete, E. Martínez-Abundis, K. G. Pérez-Rubio, M. González-Ortiz and M. M. Villar, *J. Med. Food*, 2018, **21**, 672–677.
12 N. Namazi, K. Khodamoradi, S. P. Khamechi, J. Heshmati, M. H. Ayati and B. Larijani, *Complement. Ther. Med.*, 2019, **43**, 92–101.
13 Q. Fang, S. Jiang and C. Li, *OncoTargets Ther.*, 2019, **12**, 11383–11391.
14 Y.-W. Shin, E.-A. Bae, X. F. Cai, J. J. Lee and D.-H. Kim, *Biol. Pharm. Bull.*, 2007, **30**, 197–199.
15 W.-F. Chiou, Y.-J. Sung, J.-F. Liao, A. Y.-C. Shum and C.-F. Chen, *J. Nat. Prod.*, 1997, **60**, 708–711.
16 K. L. Dong, L. Tao, J. Yang and J. J. Shang, Evodiamine decreases blood glucose in type II diabetes rats, *Basic Res. Clin. Med.*, **38**, 1443–1445.
17 E. J. Bak, H. G. Park, J. M. Kim, J. M. Kim, Y.-J. Yoo and J.-H. Cha, *Int. J. Obes.*, 2009, **34**, 250–260.
18 V. Tremaroli and F. Bäckhed, *Nature*, 2012, **489**, 242–249.
19 D. S. Wishart, *Nat. Rev. Drug Discovery*, 2016, **15**, 473–484.
20 X. Wang, J. Wu, Y. Wu, M. Wang, Z. Wang, T. Wu, D. Chen, X. Tang, X. Qin, Y. Wu and Y. Hu, *J. Diabetes Res.*, 2020, **2020**, 1–7.
21 J. Shao, Y. Liu, H. Wang, Y. Luo and L. Chen, *Oxid. Med. Cell. Longevity*, 2020, **2020**, 1–25.
22 Y. Dong, Y.-T. Chen, Y.-X. Yang, X.-J. Zhou, S.-J. Dai, J.-F. Tong, D. Shou and C. Li, *Phytother. Res.*, 2016, **30**, 823–828.
23 W. Zhou and S. Ye, *Cell Biol. Int.*, 2018, **42**, 1282–1291.
24 Y. Fan, Z. He, W. Wang, J. Li, A. Hu, L. Li, L. Yan, Z. Li and Q. Yin, *Biomed. Pharmacother.*, 2018, **106**, 733–737.
25 S. Huang, W. Peng, X. Jiang, K. Shao, L. Xia, Y. Tang and J. Qiu, *J. Diabetes Res.*, 2014, **2014**, 1–8.
26 L. Lin, S. Zhang, Y. Lin, W. Liu, B. Zou, Y. Cai, D. Liu, Y. Sun, Y. Zhong, D. Xiao, Q. Liao and Z. Xie, *J. Ethnopharmacol.*, 2020, **261**, 113013.
27 S. E. Inzucchi, R. M. Bergenstal, J. B. Buse, M. Diamant, E. Ferrannini, M. Nauck, A. L. Peters, A. Tsapas, R. Wender and D. R. Matthews, *Diabetes Care*, 2012, **35**, 1364–1379.
28 E. Said, S. Mousa, M. Fawzi, N. A. Sabry and S. Farid, *J. Adv. Res.*, 2021, **28**, 27–33.
29 J. Goletzke, C. Herder, G. Joslowski, K. Bolzenius, T. Remer, S. A. Wudy, M. Roden, W. Rathmann and A. E. Buyken, *Diabetes Care*, 2013, **36**, 1870–1876.

30 S. Zhang, Z. Yuan, H. Wu, W. Li, L. Li and H. Huang, *BioMed Res. Int.*, 2020, **2020**, 1–17.
31 M. J. Son, Y. Miura and K. Yagasaki, *Cytotechnology*, 2014, **67**, 641–652.
32 J. L. Rains and S. K. Jain, *Free Radicals Biol. Med.*, 2011, **50**, 567–575.
33 Z. Gao, Q. Lai, Q. Yang, N. Xu, W. Liu, F. Zhao, X. Liu, C. Zhang, J. Zhang and L. Jia, *Sci. Rep.*, 2018, **8**(1), 17500.
34 X. Xu, G. Yan, J. Chang, P. Wang, Q. Yin, C. Liu, Q. Zhu and F. Lu, *Oxid. Med. Cell. Longevity*, 2020, **2020**, 1–17.
35 J.-C. Tsai, Y.-A. Chen, J.-T. Wu, K.-C. Cheng, P.-S. Lai, K.-F. Liu, Y.-K. Lin, Y.-T. Huang and C.-W. Hsieh, *Molecules*, 2019, **24**, 1112.
36 S.-K. Chen, C.-H. Hsu, M.-L. Tsai, R.-H. Chen and G. Drummen, *Int. J. Mol. Sci.*, 2013, **14**, 19399–19415.
37 J. Dai, H. Ma, J. Fan, Y. Li, J. Wang, H. Ni, G. Xia and S. Chen, *Cytotechnology*, 2011, **63**, 599–607.
38 S.-M. Baek, K. Kim, S. Kim, Y. Son, H. S. Hong and S.-Y. Yu, *Sci. Rep.*, 2020, **10**(1), 16753.
39 J. J. Senn, P. J. Klover, I. A. Nowak and R. A. Mooney, *Diabetes*, 2002, **51**, 3391–3399.
40 C.-M. Yang, S.-F. Luo, H.-L. Hsieh, P.-L. Chi, C.-C. Lin, C.-C. Wu and L.-D. Hsiao, *J. Cell. Physiol.*, 2010, **224**, 516–526.
41 M. Y. Donath, M. Böni-Schnetzler, H. Ellingsgaard, P. A. Halban and J. A. Ehses, *Trends Endocrinol. Metab.*, 2010, **21**, 261–267.
42 N. Han, J. W. Chae, J. Jeon, J. Lee, H. M. Back, B. Song, K. I. Kwon, S. K. Kim and H. Y. Yun, *Nutr. Metab.*, 2018, **15**, 14.
43 I. I. A. Juvale and A. T. C. Has, *Heliyon*, 2020, **6**, e04557.
44 A. Mantovani, A. Dalbeni, D. Peserico, F. Cattazzo, M. Bevilacqua, G. L. Salvagno, G. Lippi, G. Targher, E. Danese and C. Fava, *Metabolites*, 2021, **11**, 453.
45 Z. Zheng, Z. Dai, Y. Cao, Q. Shen and Y. Zhang, *Food Funct.*, 2019, **10**, 4199–4209.
46 M. A. Glaysher, J. Ward, M. Aldhwayan, A. Ruban, C. G. Prechtl, H. L. Fisk, N. Chhina, W. Al-Najim, C. Smith, N. Klimowska-Nassar, N. Johnson, E. Falaschetti, A. P. Goldstone, A. D. Miras, J. P. Byrne, P. C. Calder and J. P. Teare, *Clin. Nutr.*, 2021, **40**, 2343–2354.
47 L. J. W. Keppley, S. J. Walker, A. N. Gademsey, J. P. Smith, S. R. Keller, M. Kester and T. E. Fox, *FASEB J.*, 2020, **34**, 15314–15326.
48 J. Prah, A. Winters, K. Chaudhari, J. Hersh, R. Liu and S.-H. Yang, *Brain Res.*, 2019, **1723**, 146378.
49 L. Zhang, J. Luo, X. Li, S. Guo and D. Shi, *Mar. Drugs*, 2020, **18**, 469.
50 K. W. Moremen, M. Tiemeyer and A. V. Nairn, *Nat. Rev. Mol. Cell Biol.*, 2012, **13**, 448–462.
51 Y. Zhong, Y. Guo, X. Liu, J. Zhang, T. Ma, J. Shu, J. Yang, J. Zhang, Z. Jia and Z. Li, *Sci. Rep.*, 2017, **7**, 45957.
52 C. Slawson, R. J. Copeland and G. W. Hart, *Trends Biochem. Sci.*, 2010, **35**, 547–555.
53 R. He, Y. Li, C. Han, R. Lin, W. Qian and X. Hou, *Int. Immunopharmacol.*, 2019, **73**, 379–388.
54 R. L. Shields, J. Lai, R. Keck, L. Y. O'Connell, K. Hong, Y. G. Meng, S. H. A. Weikert and L. G. Presta, *J. Biol. Chem.*, 2002, **277**, 26733–26740.
55 J. Li, H.-C. Hsu, Y. Ding, H. Li, Q. Wu, P. Yang, B. Luo, A. L. Rowse, D. M. Spalding, S. L. Bridges and J. D. Mountz, *Arthritis Rheumatol.*, 2014, **66**, 2368–2379.
56 A. Achari and S. Jain, *Int. J. Mol. Sci.*, 2017, **18**, 1321.
57 X. Yuan, T. Nakao, H. Satone, K. Ohara, Y. Kominami, M. Ito, T. Aizawa, T. Ueno and H. Ushio, *Nutrients*, 2020, **12**, 3798.
58 P. Tessari, D. Cecchet, A. Cosma, L. Puricelli, R. Millioni, M. Vedovato and A. Tiengo, *Clin. Nutr.*, 2011, **30**, 267–272.
59 S. Ge, Q. Zhang, Y. Tian, L. Hao, J. Duan and B. Zhang, *Clin. Chim. Acta*, 2020, **510**, 291–297.
60 K. Sumarriva, K. Uppal, C. Ma, D. J. Herren, Y. Wang, I. M. Chocron, C. Warden, S. L. Mitchell, L. G. Burgess, M. P. Goodale, M. P. Osborn, A. J. Ferreira, J. C. Law, E. F. Cherney, D. P. Jones and M. A. Brantley, *Invest. Ophthalmol. Vis. Sci.*, 2019, **60**, 3119.
61 S. M. Morris, *Annu. Rev. Nutr.*, 2002, **22**, 87–105.
62 Y.-H. You, T. Quach, R. Saito, J. Pham and K. Sharma, *J. Am. Soc. Nephrol.*, 2015, **27**, 466–481.
63 L. Zheng, S. Cardaci, L. Jerby, E. D. MacKenzie, M. Sciacovelli, T. I. Johnson, E. Gaude, A. King, J. D. Leach, R. Edrada-Ebel, A. Hedley, N. A. Morrice, G. Kalna, K. Blyth, E. Ruppin, C. Frezza and E. Gottlieb, *Nat. Commun.*, 2015, **6**, 6001.
64 J.-J. Liu, S. Liu, R. L. Gurung, J. Ching, J.-P. Kovalik, T. Y. Tan and S. C. Lim, *J. Clin. Endocrinol. Metab.*, 2018, **103**, 4357–4364.
65 W. M. Linehan and T. A. Rouault, *Clin. Cancer Res.*, 2013, **19**, 3345–3352.
66 J. S. Isaacs, Y. J. Jung, D. R. Mole, S. Lee, C. Torres-Cabala, Y.-L. Chung, M. Merino, J. Trepel, B. Zbar, J. Toro, P. J. Ratcliffe, W. M. Linehan and L. Neckers, *Cancer Cell*, 2005, **8**, 143–153.
67 W.-H. Tong, C. Sourbier, G. Kovtunovych, S. Y. Jeong, M. Vira, M. Ghosh, V. V. Romero, R. Sougrat, S. Vaulont, B. Viollet, Y.-S. Kim, S. Lee, J. Trepel, R. Srinivasan, G. Bratslavsky, Y. Yang, W. M. Linehan and T. A. Rouault, *Cancer Cell*, 2011, **20**, 315–327.
68 M. Sivashanmugam, J. Jaidev, V. Umashankar and K. N. Sulochana, *Biomed. Pharmacother.*, 2017, **86**, 185–194.
69 M. Pietzner, A. Kaul, A.-K. Henning, G. Kastenmüller, A. Artati, M. M. Lerch, J. Adamski, M. Nauck and N. Friedrich, *BMC Med.*, 2017, **15**(1), 210.
70 Y.-F. Cao, J. Li, Z. Zhang, J. Liu, X.-Y. Sun, X.-F. Feng, H.-H. Luo, W. Yang, S.-N. Li, X. Yang and Z.-Z. Fang, *Front. Endocrinol.*, 2019, **10**, 50.
71 R. S. Thandi, R. K. Radhakrishnan, D. Tripathi, P. Paidipally, A. K. Azad, L. S. Schlesinger, B. Samten, S. Mulik and R. Vankayalapati, *Nat. Commun.*, 2020, **11**(1), 3535.
72 J. L. Evans, I. D. Goldfine, B. A. Maddux and G. M. Grodsky, *Endocr. Rev.*, 2002, **23**, 599–622.
73 S.-T. Chou and S.-T. Tseng, *Clin. Exp. Nephrol.*, 2016, **21**, 283–292.

74 P. H. Whiting, A. Kalansooriya, I. Holbrook, F. Haddad and P. E. Jennings, *Br. J. Biomed. Sci.*, 2008, **65**, 71–74.
75 R. K. Sundaram, A. Bhaskar, S. Vijayalingam, M. Viswanathan, R. Mohan and K. R. Shanmugasundaram, *Clin. Sci.*, 1996, **90**, 255–260.
76 K. Murakami, K. Takahito, Y. Ohtsuka, Y. Fujiwara, M. Shimada and Y. Kawakami, *Metabolism*, 1989, **38**, 753–758.
77 R. Memısoğullari, S. Taysı, E. Bakan and I. Capoglu, *Cell Biochem. Funct.*, 2003, **21**, 291–296.
78 D. Meerza, S. Iqbal, S. Zaheer and I. Naseem, *Nutrition*, 2016, **32**, 898–903.
79 A. C. Maritim, R. A. Sanders and J. B. Watkins, *J. Biochem. Mol. Toxicol.*, 2003, **17**, 24–38.
80 O. O. Erejuwa, S. A. Sulaiman, M. S. A. Wahab, S. K. N. Salam, M. S. M. Salleh and S. Gurtu, *Int. J. Mol. Sci.*, 2011, **12**, 829–843.
81 G. D. Mattia, M. C. Bravi, O. Laurenti, M. Cassone-Faldetta, A. Armiento, C. Ferri and F. Balsano, *Metabolism*, 1998, **47**, 993–997.
82 K. Schröcksnadel, B. Wirleitner, C. Winkler and D. Fuchs, *Clin. Chim. Acta*, 2006, **364**, 82–90.
83 N. Stoy, G. M. Mackay, C. M. Forrest, J. Christofides, M. Egerton, T. W. Stone and L. G. Darlington, *J. Neurochem.*, 2005, **93**, 611–623.
84 Y. Xiao, X. Li, X. Zeng, H. Wang, Q. Mai, Y. Cheng, J. Li, L. Tang and H. Ding, *J. Agric. Food Chem.*, 2019, **67**, 7315–7324.
85 N. Sasaki, Y. Egashira and H. Sanada, *Eur. J. Nutr.*, 2009, **48**, 145–153.
86 T. Hayashi, J.-H. Mo, X. Gong, C. Rossetto, A. Jang, L. Beck, G. I. Elliott, I. Kufareva, R. Abagyan, D. H. Broide, J. Lee and E. Raz, *Proc. Natl. Acad. Sci. U. S. A.*, 2007, **104**, 18619–18624.
87 D. Krause, H.-S. Suh, L. Tarassishin, Q. L. Cui, B. A. Durafourt, N. Choi, A. Bauman, M. Cosenza-Nashat, J. P. Antel, M.-L. Zhao and S. C. Lee, *Am. J. Pathol.*, 2011, **179**, 1360–1372.
88 A. Galano, D. X. Tan and R. J. Reiter, *J. Pineal Res.*, 2011, **51**, 1–16.
89 J. Shi, D. Zhao, S. Song, M. Zhang, G. Zamaratskaia, X. Xu, G. Zhou and C. Li, *J. Agric. Food Chem.*, 2020, **68**, 6333–6346.